ELSEVIER

FEMS Microbiology Ecology 53 (2005) 285–294

FEMS MICROBIOLOGY Ecology

www.fems-microbiology.org

Dynamics in bacterial surface properties of a natural bacterial community in the coastal North Sea during a spring phytoplankton bloom

Karen Elisabeth Stoderegger *, Gerhard J. Herndl

Department of Biological Oceanography, Royal Netherlands Institute for Sea Research (NIOZ), P.O. Box 59, 1790 AB Den Burg, The Netherlands

Received 29 June 2004; received in revised form 1 January 2005; accepted 5 January 2005

First published online 26 February 2005

Abstract

The hydrophilic and hydrophobic properties of single cells of natural bacterioplankton communities were determined using a recently developed staining method combined with confocal laser scanning microscopy and advanced image analysis. On an average, about 50% of the bacterial cell area was covered by hydrophobic and only 16% by hydrophilic properties, while about 72% was covered by the genome. However, the size of these properties was independent of the bacterial cell size. Bacterial hydrophobicity was positively correlated with ambient NH_4^+ concentrations and negatively correlated with overall bacterial abundance. The expression of hydrophilicity was more dynamic. Over the spring phytoplankton bloom, the bacterioplankton $ratio_{phil/phob}$ repeatedly reached highest values shortly before peaks in bacterioplankton abundance were observed, indicating a direct and fast response of bacterial surface properties, especially hydrophilicity, to changing environmental conditions. Compared to bacterial strains, recently studied with the same method, cells of marine bacterioplankton communities are much smaller and less frequently covered by hydrophobic or hydrophilic properties. While the percentage area covered by the genome is essentially the same, the percentage area covered by hydrophobic or hydrophilic properties is much smaller.

Keywords: Bacterial cell surface; Surface properties; Hydrophobicity; Phytoplankton bloom

1. Introduction

Most actively growing and intact bacterioplankton cells exhibit a capsule as an outermost cell border [1,2] enlarging the surface and contact area of the bacterial cell with the surrounding nutrient field. The capsule consists of highly hydrated polysaccharides, polyalcohols and amino acid polymers surrounding the bacterial cell in the form of colloidal fibrils, as a slime layer or as a compact glycocalyx [3,4]. The capsule can have positively charged amino groups, negatively charged phosphate or carboxyl groups, acidic mucopolysaccharides and neutral monosaccharides like fucose or ribose [5]. In nature, the capsule of a bacterium changes quantitatively and qualitatively with its life stage [2,3]. For marine bacterioplankton communities, capsular production has been found highest during the exponential growth phase while in the stationary phase, polysaccharides attached to the outer cell surface are rapidly lost to the dissolved organic matter pool [2]. Therefore, in nature, bacterial capsular expression is linked to the environmental conditions such as nutrient availability.

Contradicting results are reported concerning the surface properties of the bacterial capsule. Hydrophobicity correlated with starvation and in nutrient-rich medium

* Corresponding author. Tel.: +31 222 369 516; fax: +31 222 319 674.
E-mail address: karen@nioz.nl (K.E. Stoderegger).

0168-6496/$22.00
doi:10.1016/j.femsec.2005.01.015

hydrophilicity were high [6]. In one study, strains without capsules were more hydrophilic [7], and in another, most electro-negative cells were capsulated [8]. Hydrophilic capsules were detected during exponential growth, however, if de-capsulated, the cells became hydrophobic [9]. Stenström and Kjelleberg [10] observed a linear relationship between high hydrophobicity and the number of fimbriated cells. These fimbriated cells also exhibited a higher negative as well as positive surface charge as compared to non-fimbriated cells [10]. Reports on bacterial surface charge frequently do not report whether bacterial capsules are present. Additionally, intensive sample manipulation may lead to a loss of the bacterial capsule.

Contradicting reports exist not only on the surface properties of the bacterial capsule but also of those of the bacterial cell wall. Hydrophobic surfaces were detected by Malmqvist [11], van Loodsrecht et al. [12] and Monger et al. [13]. All these studies report increasing hydrophobicity with increasing nutrient concentrations or activity. In contrast, increased nutrient availability was also related to more hydrophilic surfaces [14] and increased hydrophobicity was shown to be starvation-induced [15,16]. Varying nutrient concentrations are probably one of the key factors for changes in bacterial surface properties.

In a recent study using selected marine bacterial strains, we could distinguish two distinct groups of bacteria [17]. One bacterial group exhibited enhanced overall hydrophobicity, high growth rates and, at the same time, increasing hydrophobicity and hydrophilicity when growing in batch cultures. The other group was less hydrophobic, slow-growing and surface properties did not increase steadily but showed two distinct peaks in the ratio of hydrophilic to hydrophobic properties, one in the early and the other one in the late stationary phase.

Essentially, all studies on hydrophobicity of bacteria report interspecific differences [17] and differences were even noticed between individual strains of the same species [18]. Unfortunately, the results obtained with different methods to determine hydrophobicity cannot be easily compared. Common techniques to measure overall bacterial surface charge are likely to partially damage, remove, or at least, alter the delicate polysaccharide capsule and the outermost cell wall due to the intensive manipulations required prior to analysis [19].

In this study, we apply a recently developed [17] non-destructive, minimally manipulative cell surface analysis technique to quantify the hydrophobic and hydrophilic properties of individual cells from coastal bacterioplankton communities. The changes in cell surface properties were monitored and related to changes in ambient nutrient concentrations, phytoplankton abundance and the development of the bloom. The main goal of this study was therefore to determine the dynamics in hydrophobic and hydrophilic properties in a natural bacterioplankton community during the wax and wane of a phytoplankton bloom. Since bacteria represent the world's largest living surface, information on bacterial surface properties is essential to elucidate the interaction of bacteria with their environment.

2. Materials and methods

2.1. Sampling of natural bacterioplankton communities and supplementary parameters

Seawater from the coastal North Sea was taken with rinsed (0.1 N HCl) 20 l carboys from the NIOZ jetty, located at the south-west entrance of the North Sea to the Dutch Wadden Sea and characterized by strong tidal currents. Samples were taken at high tide to obtain North Sea water about twice a week between the end of March and early June 2001. Immediately after sample collection, duplicate 5 ml samples were filtered onto 0.2 μm Anodisc filters and subjected to the staining protocol described under Chapter 2.2 to determine the hydrophobic and hydrophilic moieties of the surface of individual cells of the bacterioplankton community. Additional samples were taken for chlorophyll *a* determination and inorganic nutrient analyses.

2.2. Sample preparation to quantify the hydrophobic and hydrophilic parts of the bacterial cell surface

Detection of the hydrophobic and hydrophilic parts of the bacterial cell surface was performed by applying a mixture of three fluorescent dyes to the filtered sample and subsequent confocal laser scanning microscopy (CLSM, Zeiss 510). As a polar tracer, Alexa Fluor 594 (Molecular Probes, A-10442) as a hydrophobic tracer, Dil $C_{18}(5)$ oil (25% stock solution, Molecular Probes, D-3070) in dimethylformamide and for the detection of the bacterial genome PicoGreen (Molecular Probes, P-7581) was used, a fluorescent stain mainly binding to double-stranded DNA. All three stains were stored frozen in small quantities (−20 °C) and light exposure was avoided during handling. Prior to staining the samples, the stock solutions of the stains were brought to room temperature. Per filtered sample, a working solution of 300 μl distilled water with 1.5 μl of each of the stock solutions of the three stains was prepared and thoroughly mixed. Ten millilitres of the unfixed samples was filtered onto 0.2 μm Anodisc membrane filters (Whatman, 25 mm diameter), rinsed with 0.5 ml of distilled water and after staining in the dark with the dye solution for 15 min, rinsed again twice with 0.5 ml of distilled water. The filter was transferred onto a glass slide, embedded in immersion oil (Citifluor, AF1) and

covered with a coverslip. Immediately thereafter, the sample was examined under the CLSM. Multitrack laser scanning (frame mode) to avoid fluorescence overlapping and a PlanNeofluar 100×1.3 oil objective were used for image acquisition. For the detection of genome containing cells (PicoGreen: Ex/Em: 502/523 nm), an Argon laser (488 nm) equipped with a BP 505–530 filter was used. For Alexa Fluor 594 (Ex/Em: 588/613 nm), the HeliumNeon-1 laser (543 nm) and BP 585–615 filter and for Dil $C_{18}(5)$ (Ex/Em: 644/665 nm), the HeliumNeon-2 laser (633 nm) and LP 650 were applied. Detector gain, amplitude gain and amplitude offset were adjusted only once for the whole sampling period. Thereafter, only the laser intensities were re-adjusted for each image to ensure that the gray-scale of the images never exceeded 256 (image depth: 8 Bit). During the course of the analysis, the laser intensities were standardized regularly as described below.

2.3. Image analysis

For a detailed description of the image analysis protocol, the reader is referred to Stoderegger and Herndl [17]. For image analysis, the Zeiss KS 300 software package was applied. On the composite three-channel image, the area of each individual bacterial cell was determined and subsequently, the threshold levels for the three channels were adjusted separately for this area. The images were checked for detected cells and eventually corrected by excluding or adding cells originally not detected by the channel settings. The total area as well as the partial area and its mean fluorescence intensity for each of the three channels were determined. The mean fluorescence intensity of the specific stain represents the average fluorescence per specific area normalized to 100% laser intensity. Per sample, 15 images (10–30 bacteria per image) were taken in total.

The hydrophobic and hydrophilic properties of individual cells are expressed as $\mathrm{IND}_{\mathrm{prop}}$. This index relates the area to the mean fluorescence intensity of the hydrophobic or hydrophilic properties and was calculated separately for each property, where $_{\mathrm{prop}}$ stands for hydrophilic or hydrophobic property of the individual bacterial cell. $\mathrm{IND}_{\mathrm{prop}}$ was calculated as follows:

$$\mathrm{IND}_{\mathrm{prop}} = (D_{\mathrm{prop}}/D_{\mathrm{prop,ave}}) \times \mathrm{AR}_{\mathrm{prop}}, \quad (1)$$

where D_{prop} and $\mathrm{AR}_{\mathrm{prop}}$ are the mean fluorescence intensity and the specific area (expressed as percentage of total area) of the individual cell, respectively, and $D_{\mathrm{prop,ave}}$ is the mean fluorescence intensity of all the cells examined on the filter. As fluorescence intensity is not an absolute value, we standardized the laser intensity to the average fluorescence of the analyzed bacteria to allow comparison of fluorescence intensities among different samples. To include cells lacking fluorescence indicative for a specific property in the assessment of the total bacterial community, we calculated community indices for the specific properties

$$\mathrm{COM}_{\mathrm{prop}} = (\mathrm{IND}_{\mathrm{prop,ave}} \times N_{\mathrm{prop}})/N_{\mathrm{tot}}, \quad (2)$$

where N_{prop} is the number of bacteria exhibiting the specific property and N_{tot} is the total number of bacteria. $\mathrm{IND}_{\mathrm{prop,ave}}$ is the average value of $\mathrm{IND}_{\mathrm{prop}}$ derived from Eq. (1). A $\mathrm{COM}_{\mathrm{prop}}$ of 100 would therefore indicate a community where the whole area of the individual cells is occupied by the specific property exhibiting the average of the mean fluorescence intensity per cell. Additionally, a surface property index, represented by the ratio between hydrophilic and hydrophobic properties ($\mathrm{ratio}_{\mathrm{phil/phob}}$), was calculated by

$$\mathrm{ratio}_{\mathrm{phil/phob}} = \mathrm{COM}_{\mathrm{hydrophilic}}/\mathrm{COM}_{\mathrm{hydrophobic}}. \quad (3)$$

2.4. Standard preparation

The stability of the laser over time and the linearity of the fluorescence signal with increasing laser intensity were checked with standard fluorescent beads (InSpeck, $\Phi = 2.5$ μm, 0.3% relative fluorescence, Molecular Probes, I-7219, I-7224, I-7225). These fluorescent beads were tested periodically under the specific CLSM setting using the single-track option from the lowest possible (minimum gray-scale >20) to the highest possible laser intensity (maximum gray-scale 256). For the Argon laser (488 nm) InSpeck Green (Ex/Em: 505/515 nm), for the HeliumNeon-1 laser (543 nm) InSpeck Red (Ex/Em: 580/605 nm), and for the HeliumNeon-2 laser (633nm) InSpeck Deep Red (Ex/Em: 633/660 nm) were used. For the whole sampling period, the correlation coefficients of the linear regression for the three different standard fluorescent beads were $r^2 = 0.96$ for InSpeck Red ($n = 420$), $r^2 = 0.93$ for InSpeck Deep Red ($n = 438$) and for InSpeck Green $r^2 = 0.94$ ($n = 255$).

2.5. Additional parameters

For chlorophyll *a* (chl *a*) determinations, 500–700 ml of freshly collected seawater was filtered onto a Whatman GF/F filter, stored at −20 °C and chl *a* and pheopigment concentrations were determined according to Yentsch and Menzel [20]. Also, water samples were taken for inorganic nutrients (described below). For inorganic nutrient analyses (NH_4^+, NO_3^-, NO_2^-, PO_4^{3-}), samples were frozen after gentle filtration through 0.2 μm filters (Acrodisc, Gelman Science) and stored at −20 °C until analysis in a TRAACS autoanalyzer system. NH_4^+ was detected with the indo-phenolblue-method (pH 10.5) at 630 nm wavelength [21]. NO_2^- was detected after diazotation with sulphanilamide and *N*-(1-naphthyl)-ethylene diammonium-dichloride as the reddish-purple dye complex at 540 nm wavelength [22]. NO_3^- was reduced in a copper cadmium coil to nitrite

(using imidazole as a buffer) and then measured as nitrite. Inorganic phosphate was determined via the molybdenum blue complex at 880 nm wavelength according to Murphy and Riley [23]. Samples for the determination of silicate were stored at 4 °C until analysis after filtration through 0.2 μm filters (Acrodisc, Gelman Science). Ascorbic acid was used as reducing agent and oxalic acid to prevent interference of phosphate. Finally, dissolved silicate was measured as a blue reduced silicomolybdenium complex at 810 nm wavelength [24].

3. Results

3.1. Cell characteristics of natural bacteria

To determine the overall cell characteristics of natural bacterioplankton communities, the datasets of different bacterial parameters of all sampling dates were pooled and related to each other and to cell size (Tables 1 and 2). In total, we counted 7292 cells of which 94% were detected by PicoGreen, thus leaving 6% of ghost cells, and 90% showed hydrophobic and 36% exhibited hydrophilic moieties (Table 1). Bacterial cells covered, on average, an area of 0.9 μm^2, of which 72% was covered by the genome and 55% of the total cell area was covered by hydrophobic and 16% by hydrophilic moieties (Table 1).

Table 1
Cell characteristics of coastal North Sea bacterial communities as determined by fluorescent stains for DNA, hydrophobic and hydrophilic surface properties

	Total	Genome	Hydrophobic	Hydrophilic
Counts	7292	6847	543	2591
	100%	93.9%	89.7%	35.5%
Area (μm^2)	0.90 ± 0.51	0.65 ± 0.44	0.51 ± 0.37	0.18 ± 0.23
	100%	71.9 ± 23.4%	54.9 ± 24.8%	16.1 ± 16.5%
Intensity		6726 ± 62	2770 ± 354	1028 ± 129

Absolute numbers and the percentage of the total are given. Areas and mean intensities (± standard deviation) of the specific properties are significantly different from each other (*t* test for dependent samples, $p < 0.001$, n = see counts, actual number of observations).

With increasing cell size, the genome-stained area as well as the hydrophobic and the hydrophilic area of the cell increased (Table 2A). This increase, as indicated by the slope (k) of the linear regression, was lowest for the hydrophilic area ($k = 0.17$) and 3 times higher for the hydrophobic area ($k = 0.51$) and highest for the genome area ($k = 0.69$). The three slopes were significantly different from each other (comparison for homogeneity of slopes for all combinations, $p < 0.01$).

Mean fluorescence intensities of the hydrophobic and hydrophilic regions were independent of the cell size (Table 2A), while specific mean genome fluorescence intensity was related to the corresponding area ($r = 0.32$, $p < 0.05$, $n = 6847$) (Table 2A). When comparing the areas or the mean intensities of the specific moieties with each other, significant correlations (with higher correlation coefficients for mean intensities) were detectable (Table 2B) indicating concomitant changes of the different moieties. The slopes for genome to hydrophobic area, genome to hydrophilic area and hydrophobic to hydrophilic area were $k = 0.54$, $k = 0.13$, and $k = 0.13$, respectively, and were significantly different from each other (comparison for homogeneity of slopes, $p < 0.05$).

To relate hydrophobic or hydrophilic areas with the corresponding mean fluorescence intensities, relative indices, $IND_{hydrophobic}$ and $IND_{hydrophilic}$ (Eq. (1)), for the individual cells were determined. Subsequently, these indices were related to total bacterial cell size. If percent values for the area were used in Eq. (1), changes of hydrophobic and hydrophilic properties were found to be independent of bacterial cell size (correlation, $r^2 < 0.01$ for $n = 6543$, $n = 2591$ for hydrophobic and hydrophilic properties). If absolute values were used, however, hydrophobic and hydrophilic indices increased with cell size (correlation, $r^2 = 0.52$, $n = 6543$ and $r^2 = 0.22$, $n = 2591$ for hydrophobic and hydrophilic properties). The overall higher $IND_{hydrophobic}$ than

Table 2
Pearson's correlation coefficients (r) of the specific bacterial characteristics (number of observations are given in brackets)

	Genome (6847)	Hydrophobic (6543)	Hydrophilic (2591)
A			
Total cell area to specific area	0.81	0.73	0.45
Total cell area to specific intensity	0.19	n.s.	0.09
Specific area to specific intensity	0.41	n.s.	0.1

	Hydrophobic intensity	Genome intensity	Hydrophobic area	Genome area	
B					
Hydrophobic intensity		0.41		0.61	Hydrophobic area
Hydrophilic intensity	0.40	0.63	0.24	0.29	Hydrophilic area

In (A) total cell area is compared with the specific properties and specific areas are compared to their specific intensities, whereas in (B) surface properties are compared within each other. Correlations with $p < 0.01$ are shown, n.s.-not significant.

$IND_{hydrophilic}$ is mainly due to the smaller hydrophilic than hydrophobic areas.

3.2. Temporal changes in bacterioplankton cell surface properties during spring phytoplankton bloom

The dynamics in cell surface properties of the bacterioplankton communities during a spring bloom were followed and related to the changing environmental parameters such as chl *a* and nutrient concentrations.

During the first two weeks of the sampling campaign, total chl *a* concentration was high (10–5 μg l^{-1}) due to a diatom-dominated bloom accounting for 80–90% of the total chl *a* (Fig. 1) as revealed by HPLC pigment analysis (data not shown). This bloom was followed by two subsequent diatom-dominated (60–70% and 65–75% of the total chl *a*, respectively) blooms, succeeded by a *Phaeocystis*-dominated bloom with a maximum chl *a* concentration of 29 μg l^{-1} (Fig. 1).

The following analysis focuses on the diatom-dominated blooms, as only a few data are available for the *Phaeocystis* bloom. Unless stated otherwise, statistical analysis was performed using time series analysis by cross-correlation (Statistica 6). Total bacterial abundance was, on average, $17.5 \pm 8.7 \times 10^5$ cells ml^{-1} and varied between 7.0 and 36×10^5 cells ml^{-1} following the dynamics of chl *a* with a time lag of 5 d ($r = 0.86$, $n = 28$, $p < 0.05$, Fig. 1, Table 3). During the entire sampling period, the abundance of cells exhibiting hydrophobicity varied between 78.6% and 96.3% (mean ± SD: 90.2 ± 5.1%) of total bacterial abundance. The abundance of cells exhibiting hydrophobicity correlated well ($r = 0.99$, $n = 28$, time lag = $c\backslash 0$, $p < 0.05$) with total bacterial abundance. The abundance of cells exhibiting hydrophilicity varied between 7.6% and 77.2% (40.1 ± 21.0%) of total bacterial abundance and followed the dynamics of bacterial abundance and the abundance of cells exhibiting hydrophobicity with a time lag of 7 days ($r = 0.45$ and $r = 0.41$, $p < 0.05$, respectively).

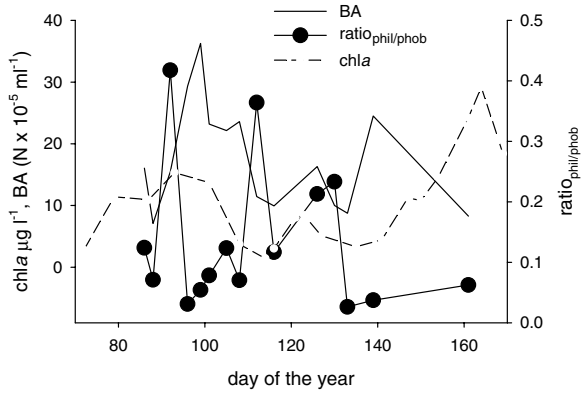

Fig. 1. Temporal dynamics of chlorophyll *a* (chl *a*), bacterial abundance (BA) and the $ratio_{phil/phob}$ during a phytoplankton bloom in the coastal North Sea in the spring of 2000.

Table 3
The correlation coefficient (*r*) for the different parameters as determined by time series analysis (cross correlation; $n = 28$, for comparisons between bacterial and chl *a*-measurements $n = 45$) is shown

Pattern	Total cell area	Genome area	Hydrophobic area	Chl *a*
Genome area	0.78		–	n.s.
Hydrophobic area	0.53	0.83	–	−0.45
Hydrophilic area	0.51	0.53 (−15)	n.s.	n.s.
Bacterial abundance	n.s.	−0.59	−0.7 (1)	0.86 (5)

Absolute values of the different areas are compared. The time lag is usually 0 day, otherwise stated in parentheses.

During the sampling period, between 50.5% and 88.9% (76.2 ± 12%) of the cell area was covered by the genome thus covering about 1.5-times more area than hydrophobic (56.9 ± 8.4%) and 6-times more than hydrophilic (15.5 ± 5.3%) moieties (*t* test, $p < 0.05$, $n = 30$). The hydrophilic area was more dynamic over time (SD = 38% of the mean) than the hydrophobic, genome or total cell area (SD = 14%, 22%, 14% of the mean, respectively). Over the entire sampling period, the correlation of the mean total cell area with mean genome area was higher ($r = 0.78$, $n = 26$, $p < 0.05$) than its correlation with mean hydrophobic ($r = 0.53$, $n = 26$, $p < 0.05$) or mean hydrophilic ($r = 0.51$, $n = 26$, $p < 0.05$) area (Table 3). Mean genome area was positively correlated with mean hydrophobic area ($r = 0.83$, $n = 26$, $p < 0.05$) and both were negatively correlated with bacterial abundance (Table 3). Mean hydrophobic area was negatively correlated with chl *a* (Table 3).

The surface property index, expressed as the $ratio_{phil/phob}$, varied between 0.03 and 0.4 (0.07 ± 0.036, $n = 11$), i.e., more than 10-fold over the sampling period (Fig. 1). Three distinct peaks in the $ratio_{phil/phob}$ were noticed, before and after the diatom-dominated bloom (Fig. 1). The $ratio_{phil/phob}$ was negatively correlated with total bacterial abundance ($r = -0.47$, time lag 1 day, $n = 26$, $p < 0.05$) and with mean total cell size ($r = 0.63$, time lag 0 day, $n = 26$, $p < 0.05$). Furthermore, the $ratio_{phil/phob}$ correlated better with the hydrophilic community index, $COM_{hydrophilic}$ ($r = 0.95$, time lag 0 day, $n = 26$, $p < 0.05$) than with the hydrophobic community index, $COM_{hydrophobic}$ ($r = 0.58$, time lag −5 days, $n = 26$, $p < 0.05$).

$COM_{hydrophobic}$ varied between 35.4 and 73.7 and showed a similar trend as NH_4^+ ($r = 0.82$, time lag 0 d, $n = 26$, $p < 0.05$) (Fig. 2), while it was negatively related to chl *a* ($r = -0.7$, time lag 0 d, $n = 26$, $p < 0.05$) and to NO_3^- with a time lag of 4 d ($r = -0.58$, $n = 26$, $p < 0.05$). $COM_{hydrophilic}$ varied between 1.1 and 17.1 and was generally poorly correlated with phytoplankton related parameters (NH_4^+: $r = 0.45$, time lag −7 d, chl *a* : $r = -0.48$, time lag −3 d, NO_3: $r = -0.42$, time lag −9 d, for all: $n = 26$, $p < 0.05$) (Fig. 2). $COM_{hydrophobic}$

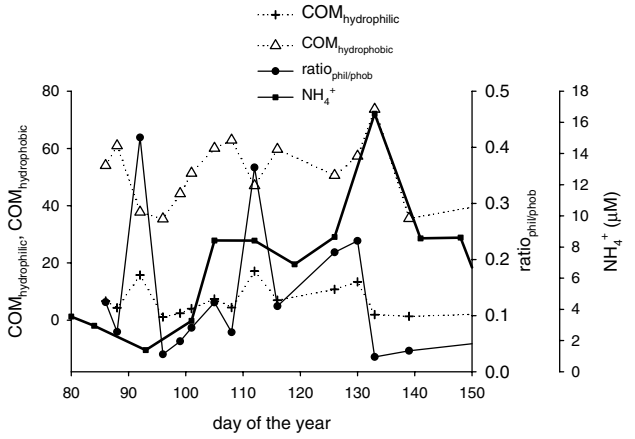

Fig. 2. Variation of bacterial surface properties ($COM_{hydrophobic}$, $COM_{hydrophilic}$ and the $ratio_{phil/phob}$) and NH_4^+ concentration at the study site during the sampling period.

and $COM_{hydrophilic}$ were negatively correlated with bacterial abundance ($r = -0.59$, $r = -0.58$, time lag -3 d and -1 d, respectively, $n = 28$, $p < 0.05$).

Using principal component analysis, calculated from the main correlating variables of the normalized dataset, four principal components (PCs) showed eigenvalues >1 explaining 87.9% of the total variance (Table 4). The first two principal components, PC1 and PC2, explained 58% of this variance and were related to parameters indicative for phytoplankton biomass and activity. Inorganic nutrients, especially nitrogen availability, were the driving force showing highest loading with PC1, which explained 31% of the variability. About the same rate of variability (27%) was explained by PC2, consisting of variables more directly related to phytoplankton (e.g., chl *a*, diatoms). PC3 and PC4 summarized information on bacterial related parameters, such as bacterial abundance and surface properties and together explained one third of the variance. The randomization procedure (Covran) testing the significance of the factor loading confirmed that the factor loading of the characters used to interpret principal components were significant in all cases (Table 4).

Table 4
The loading of the original variables for the first four principal components and the percentage of explained variance

Variables	Factor loadings			
	PC1 30.7%	PC2 27.2%	PC3 15.8%	PC4 14.1%
NO_3^-	**0.9**	−0.13	−0.09	0.24
NH_4^+	**−0.8**	−0.25	0.05	0.14
Dissolved silica	**0.77**	**−0.55**	−0.1	0.2
PO_4^{3-}	**0.48**	**−0.66**	−0.18	0.04
Chl *a*	0.25	**−0.86**	−0.3	0.2
Diatoms	0.25	**−0.87**	−0.3	0.2
Bacterial abundance	0.38	0.27	**0.81**	−0.15
$COM_{hydrophilic}$	−0.03	−0.11	**−0.69**	**−0.68**
$COM_{hydrophobic}$	−0.46	−0.23	−0.24	**0.76**

Significant factor loadings (randomization procedure: Covran) of the characters used to interpret principal components are given in bold.

4. Discussion

This and an earlier study [17] are the only reports thus far measuring bacterial hydrophobicity and hydrophilicity simultaneously by use of molecular probes. A discussion on the potential and limitations of this method is given in detail in Stoderegger and Herndl [17]. Using two fluorescent stains for tracing surface properties, we were able to simultaneously measure the hydrophobicity and polar moieties of the bacterial cell surface. Hydrophilic areas were usually smaller than hydrophobic areas and non-hydrophilic cells were encountered more frequently than non-hydrophobic cells. This is probably due to the fact that the hydrophobic stain is binding to the lipid bilayer of the cell wall, the lipopolysaccharides of the outer membrane and the capsule, or other structures of the cell wall and membrane, while the hydrophilic stain is targeting mainly the latter two surface moieties.

One major drawback of the method might be that such probes eventually intercalate within the cell envelope and may bind to sites not only located at the outermost cell surface but also intracellularly. The molecular size of the stains used in this study (760 and 960 Da for the hydrophilic and hydrophobic stain, respectively) is slightly higher than the average size of molecules which can pass the Gram-negative bacterial cell wall (≈600 Da) [25]. We thus assume that the stains used in this study are staining predominantly the outer parts of the cell and do not penetrate the cell wall.

As pretreatment of the samples is minimized with the method presented here, the risk of major losses or changes of the outermost cell surface is low. We obtained relative fluorescence values for specific properties and area values are indicating the total cell area covered by the specific property. The weak correlation of the specific fluorescence to the specific area, especially for hydrophilic and hydrophobic properties (see Table 2A), indicates heterogeneity among different members of natural bacterial assemblages. For area detection with the CLSM, Sieracki et al. [26] found that the visual threshold determination, as used in this study, tends to overestimate the threshold, causing an underestimation of microsphere size. Only for the smallest and brightest fluorescing cells, these authors reported an overestimation of the actual cell size (in their case *Synechococcus* sp.). The microspheres we used (2.5 μm diameter) for standardization usually indicated that we slightly overestimated their size (∼2.7 ± 0.2 μm, for all the different beads).

Due to the lack of an absolute unit for hydrophobicity, essentially all studies on the hydrophobicity of bacterial cell surfaces used relative units making comparison among different methods difficult.

4.1. Individual surface properties

Marine bacterial strains, mainly isolated from the Atlantic and growing in batch cultures [17], were usually significantly larger than cells of natural communities (2.1 ± 1.3 vs. 0.9 ± 0.5 μm^2, respectively, t test for independent samples, $p < 0.01$, $n = 7292$, $n = 13243$). The portion covered by the genome (~72% for both), however, is essentially the same (Fig. 3(a)).

With regard to hydrophobicity, 95% of the bacterial strains in batch cultures were covered to 77% by hydrophobic properties (Fig. 3(b)), while 90% of the natural community (Table 1) was covered to 55% by hydrophobic properties (t test for independent samples, $p < 0.01$, $n = 12638$, $n = 6544$, Fig. 3(b)).

Hydrophilic properties were found in 36% of seawater bacteria covering 16% of the area (Fig. 3(c), Table 1), while 52% of cultured bacteria (Fig. 3(c)) were covered up to 30% by hydrophilic properties (t test for independent samples, $p < 0.01$, $n = 2592$, $n = 6818$). This is about twice the surface area reported to be covered by hydrophilic properties found in one other study [27]. These authors calculated that charged groups occupy only a minor fraction (8%) of the total surface area, assuming that all charge is caused by carboxyl groups at the outer surface. As this study did not use a staining technique, these results cannot be directly compared.

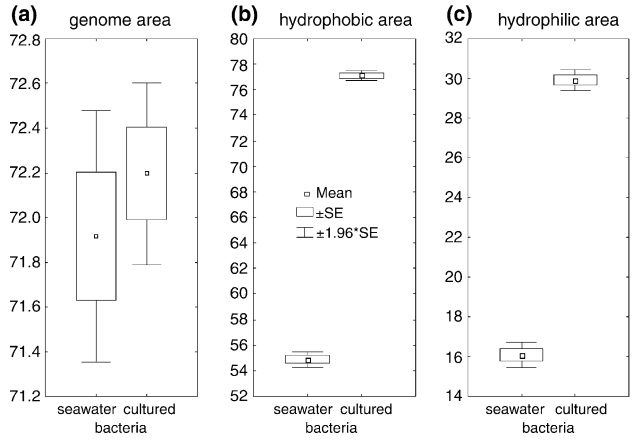

Fig. 3. Differences between natural bacterioplankton communities of the North Sea (seawater) and the pooled data set of culture experiments with six different strains (cultured) expressed as the percentage of the total cell size covered by: (a) the genome area, (b) hydrophobic area, and (c) the hydrophilic area. For (a) $n = 6847$ and $n = 10,747$ for (b) $n = 6543$ and $n = 12,637$ and for (c) $n = 2591$ and $n = 6817$, for natural bacterial communities and for cultured bacteria, respectively. Data on the bacterial strains are from Stoderegger and Herndl [17].

Obviously, cultured bacteria are on average larger and, independent of the size of the bacteria, express more extensively hydrophobic and hydrophilic properties as compared to natural bacterial communities. On one hand, this can be a result of permanent removal of larger and faster growing bacteria from natural communities due to attachment or grazing [28]. On the other hand, enhanced nutrient availability could enable cultured bacteria to express surface moieties more intensively. Many authors have attributed the enlargement of cells under cultured conditions to increased nutrient availability [29,30]. The results obtained in this study and on bacterial strains [17] support this hypothesis. In contrast, Kjelleberg and Hermansson [31] found consistently higher hydrophobicity in nutrient-deprived cells and interpreted this as a mechanism of the bacterial cell to survive starvation.

4.2. Surface properties and cell size

The portion of the bacterial cell surface that is hydrophobic or hydrophilic, expressed as $IND_{hydrophobic}$ and $IND_{hydrophilic}$, respectively, is not related to cell size in natural bacterial communities, a pattern also found for cultured bacteria [17]. Still, it is quite obvious that cultured bacteria, despite being about twice as large as bacteria in situ and expressing about the same relative amount of genome (72%, Fig. 3(a)), exhibit significantly more hydrophilic (nearly twice as much) as well as hydrophobic properties than cells of natural communities (Fig. 3(b) and (c)). Culture conditions differ from natural conditions regarding nutrient availability and grazing pressure. As discussed above, the overall enlargement of cultured cells is probably due to favorable nutrient conditions.

4.3. Dynamics of bacterial surface properties during a phytoplankton bloom

Bacterial hydrophobicity was negatively correlated without time lag with the concentration of chl *a* (Table 3) and positively ($r = 0.82$, cross correlation) with the concentration of NH_4^+ (see also Fig. 2). Thus, there is evidence that bacteria are more hydrophobic when regenerated nitrogen concentrations are high. Three explanations for this phenomenon can be offered. In the presence of NH_4^+, bacterial species with a higher capacity to express hydrophobicity might develop, better adapted to utilize this nitrogen source. Although no direct links with PO_4^{3-} could be demonstrated, an increase of organic phosphorus induced by a decaying phytoplankton bloom could favor hydrophobic bacteria readily taking up dissolved organic phosphorus [14]. It is unlikely that this is the only mechanism responsible for the observed pattern, because bacterial abundance and hydrophobicity are negatively linked

to each other ($r = -0.6$, time lag = 3 d, cross correlation). Furthermore, the development of more hydrophobic bacterial species in the presence of NH_4^+ should involve a time lag between NH_4^+ and hydrophobicity. A decrease in less hydrophobic bacterial species would have the same effect on the observed overall increase in hydrophobicity of the bacterial community. Less hydrophobic bacteria might be removed by grazing resulting in the enhanced production of NH_4^+. For the same study site, Arrieta and Herndl [32] reported a decreased bacterial richness after a phytoplankton bloom and Gurijala and Alexander [33] found that species that persisted at high abundance had highly hydrophobic cell surfaces.

Originally less hydrophobic bacteria could also become more hydrophobic by changing the composition of surface molecules. NH_4^+ could be adsorbed to the negatively charged groups of the amphiphilic polysaccharides [5] rendering bacteria more hydrophobic (mask effect). Thus, NH_4^+ availability and hydrophobicity might be directly linked. Bacterioplankton hydrophobicity decreased from the upper 80 m water column to deeper layers, where NH_4^+ concentrations are usually low [13]. Hydrophobicity was also found to increase with increased dilution rates in continuous cultures, whereas electrophoretic mobility did not change markedly [27]. Cationic quaternary ammonium salts have been found to interact with biological and model membranes [34,35]. Since $COM_{hydrophobic}$ and $COM_{hydrophilic}$ are positively correlated ($r = 0.42$, $n = 28$, $p < 0.05$), increased hydrophobicity is accompanied by an increase in hydrophilicity. From the present results, it remains unclear whether the variation in bacterioplankton hydrophobicity resulted from a genotypic shift due to differential growth, from grazing mortality of individual genotypes or from a phenotypic response of the community to changes in the chemical environment.

Several authors have demonstrated an increase of hydrophobicity during the growth phase in culture experiments [11,12,36,37], whereas other marine isolates were found more hydrophobic during starvation [15,31]. van Loodsrecht et al. [27] concluded that coastal bacteria tend to adhere to surfaces under optimal growth conditions, while for open ocean bacteria attachment to particles enhances the chance of bacteria to be vertically transported [27].

Although most of the above-mentioned studies suggest increased hydrophobicity during exponential growth, bacterial abundance was negatively correlated with hydrophobicity and hydrophilicity ($r = -0.59$, $r = -0.58$ cross correlation) with a time lag of 3 d. Grazing might therefore play a role in the expression of surface properties in the bacterioplankton communities. Hydrophobicity has been suggested as a mechanism of bacterial cells to reduce grazing pressure [33]. This is in contrast to the above suggestion that larger bacteria or bacteria with a higher surface charge should be grazed more efficiently. No correlation of bacterial abundance with bacterial size could be found (Table 3). Also, mean hydrophobic and genome area were negatively correlated with bacterial abundance (Table 3) supporting the hypothesis that the overall smaller size and lower surface properties of bacteria in their natural environment are caused by the overall lower nutrient concentration in situ as compared to culture conditions, rather than by grazing. This conclusion is supported by Matz and Jürgens [34] who did not find any correlation between grazing rates of flagellates and the surface charge of their bacterial prey.

4.4. Dynamics in the surface property index

The dynamics in the surface property index, the $ratio_{phil/phob}$, are depending more on the variations in hydrophilicity (Fig. 2, $r = 0.95$, time lag = 0 d, cross correlation) rather than on the variability of hydrophobicity. This is indicated by the peaks in the $ratio_{phil/phob}$ (Fig. 2), which were mainly caused by an increase in hydrophilicity and a corresponding smaller decrease of hydrophobicity. A similar pattern was observed in cultures of *Acinetobacter calcoaceticus*. Cells in the early stationary phase are hydrophobic and as the medium becomes nutrient depleted, emulsan, a polysaccharide with fatty acids distributed along the entire length of the molecule, accumulates as a minicapsule at the cell surface, decreasing hydrophobicity again. In the late stationary phase, the capsular polymer is released into the medium and the cells become hydrophobic again [35]. In our previous batch culture study [17], we were able to differentiate two groups of bacteria based on their surface property index. One group, characterized by generally high hydrophobicity and high growth rates, exhibited a continuous increase in the $ratio_{phil/phob}$ during growth in batch cultures. The less hydrophobic group of bacterial strains exhibited two peaks in this ratio, one at the transition from the exponential growth phase to the stationary phase and the other in the senescent stage. The natural bacterial communities studied here belong to the second group of bacteria, due to their overall low hydrophobic and hydrophilic community indices. This group also showed lower growth rates, suggesting that bacteria are better adapted to lower nutrient concentrations. Although these bacterial groups (*Alteromonas*, *Pseudoalteromonas*, *Vibrio*-populations) are readily culturable, they exhibit a remarkably low abundance in situ [36]. Beardsley et al. [37] demonstrated that although these groups of bacteria show high growth rates in cultures, they over-proportionally decline during the increase in flagellate abundance, in contrast to members of the *Roseobacter* group.

In conclusion, we show in this study that coastal North Sea bacterioplankton express less surface properties

than marine bacterial strains in batch cultures. Hydrophobicity is enhanced when regenerated nitrogen concentrations are elevated and bacterial abundance is low, suggesting that hydrophobicity is a means to reduce grazing pressure.

Acknowledgments

We thank Anna Noordeloos for providing the chl *a* data and Gerhard Cadee and Katja Phillipard for providing the nutrient data. Financial support was provided by the Royal Netherlands Institute for Sea Research (NIOZ), by a post-doctoral grant from the Austrian Science Foundation (FWF) to K.E.S and by the 5th Framework Program of the Commission of the European Community via the BASICS project.

References

[1] Kennedy, A.F.D. and Sutherland, I.W. (1987) Analysis of bacterial exopolysaccharides. Biotechnol. Appl. Biochem. 9, 12–19.
[2] Stoderegger, K. and Herndl, G.J. (1998) Production and release of bacterial capsular material and its subsequent utilization by marine bacterioplankton. Limnol. Oceanogr. 43, 877–884.
[3] Decho, A.W. (1990) Microbial exopolymer secretions in ocean environments: their role(s) in food webs and marine processes. Oceanogr. Mar. Biol. Ann. Rev. 28, 73–153.
[4] Heissenberger, A., Leppard, G.G. and Herndl, G.J. (1996) Relationship between the intracellular integrity and the morphology of the capsular envelope in attached and free-living marine bacteria. Appl. Environ. Microbiol. 62, 4521–4528.
[5] Kenne, L. and Lindberg, B. (1983) Bacterial polysaccharides In: The Polysaccharides (Aspinall, G.O., Ed.), pp. 287–363. Academic Press, New York.
[6] Singh, K.K. and Vincent, W.S. (1987) Clumping characteristics and hydrophobic behavior of an isolated bacterial strain from sewage sludge. Appl. Microbiol. Biotechnol. 25, 396–398.
[7] Meno, Y. and Fujimoto, S. (2002) Characteristics of capsules in enterotoxemic *E. coli* O139:K12 strains causing swine edema disease. Microbiol. Res. 157, 1–5.
[8] Bayer, M.E. and Bayer, M.H. (1994) Biophysical and structural aspects of the bacterial capsule. ASM News 4, 192–198.
[9] Rosenberg, E., Kaplan, N., Pines, O., Rosenberg, M. and Gutnick, D. (1983) Capsular polysaccharides interfere with adherence of *Actinobacter calcoaceticus* to hydrocarbon. FEMS Microbiol. Lett. 17, 157–160.
[10] Stenstroem, T.-A. and Kjelleberg, S. (1985) Fimbria mediated nonspecific adhesion of *Salmonella typhimurium* to mineral particles. Arch. Microbiol. 143, 6–10.
[11] Malmqvist, T. (1983) Bacterial hydrophobicity measured as partition of palmitic acid between the two immiscible phases of cell surface and buffer. Acta Pathol. Microbiol. Immunol. Scand. Sect. B 91, 69–73.
[12] van Loodsrecht, M.C.M., Lyklema, J., Norde, W., Schraa, G. and Zehnder, A.J.B. (1987) The role of bacterial cell wall hydrophobicity in adhesion. Appl. Environ. Microbiol. 53, 1893–1897.
[13] Monger, B.C., Landry, M.R. and Brown, S.L. (1999) Feeding selection of heterotrophic marine nanoflagellates based on the surface hydrophobicity of their picoplankton prey. Limnol. Oceanogr. 44, 1917–1927.
[14] Lemke, M.J., Churchill, P.F. and Wetzel, R.G. (1995) Effect of substrate and cell surface hydrophobicity on phosphate utilization in bacteria. Appl. Environ. Microbiol. 61, 913–919.
[15] Dawson, M.P., Humphrey, B.A. and Marshall, K.C. (1981) Adhesion: a tactic in the survival strategy of a marine vibrio during starvation. Curr. Microbiol. 6, 195–199.
[16] Wrangstadh, M., Szewzyk, U., Östling, J. and Kjelleberg, S. (1990) Starvation-specific formation of a peripheral exopolysaccharide by a marine *Pseudomonas* sp., strain S9. Appl. Environ. Microbiol. 56, 2065–2072.
[17] Stoderegger, K.E. and Herndl, G.J. (2004) Dynamics in bacterial cell surface charge assessed by fluorescent stains and confocal laser scanning microscopy. Aquat. Microb. Ecol. 36, 29–40.
[18] Jana, T.K., Srivastava, A.K., Csery, K. and Arora, D.K. (2000) Influence of growth and environmental conditions on cell surface hydrophobicity of *Pseudomonas fluorescens* in non-specific adhesion. Can. J. Microbiol. 46, 28–37.
[19] Pembrey, R., Marshall, K.C. and Schneider, R.P. (1999) Cell surface analysis techniques: what do cell preparation protocols do to cell surface properties?. Appl. Environ. Microbiol. 65, 2877–2894.
[20] Yentsch, C.S. and Menzel, D.W. (1963) A method for the determination of phytoplankton chlorophyll and phaeophytin by fluorescence. Deep-Sea Res. 10, 221–231.
[21] Helder, W. and Vries, R.d. (1979) An automatic phenol-hypochlorite method for the detection of ammonia in sea- and brackish waters. Netherlands J. Sea Res. 13, 154–160.
[22] Parsons, T.R., Maita, Y. and Lalli, C.M. (1984) A Manual of Chemical and Biological Methods for Seawater Analysis. Pergamon Press, Oxford, 173 pp.
[23] Murphy, J. and Riley, J.P. (1962) A modified single solution method for the determination of phosphate in natural waters. Anal. Chim. Acta 27, 31–36.
[24] Strickland, J.D.H. and Parsons, T.R. (1972) A practical handbook of seawater analysis. Fisheries Res. Board Canada, Bull. 167, 310 pp.
[25] Payne, J.W. (1980) Transport and utilization of peptides by bacteria In: Microorganisms and Nitrogen Sources (Payne, JW, Ed.), pp. 212–256. Wiley, New York.
[26] Sieracki, M.E., Reichenbach, S.E. and Webb, K.L. (1989) Evaluation of automated threshold selection methods for accurately sizing microscopic fluorescent cells by image analysis. Appl. Environ. Microbiol. 55, 2762–2772.
[27] van Loodsrecht, M.C.M., Lyklema, J., Norde, W., Schraa, G. and Zehnder, A.J.B. (1987) Electrophoretic mobility and hydrophobicity as a measure to predict the initial steps of bacterial adhesion. Appl. Environ. Microbiol. 53, 1898–1901.
[28] Del Giorgio, P.A., Gasol, J.M., Vaque, D., Mura, P., Agusti, S. and Duarte, C.M. (1996) Bacterioplankton community structure: protists control net production and the proportion of active bacteria in a coastal marine community. Limnol. Oceanogr. 41, 1169–1179.
[29] Ammerman, J.W., Fuhrman, J.A., Hagström, Å and Azam, F. (1984) Bacterioplankton growth in seawater: I. Growth kinetics and cellular characteristics in seawater cultures. Mar. Ecol. Prog. Ser. 18, 31–39.
[30] Kato, K. (1996) Image analysis of bacterial cell size and diversity In: Microbial Diversity in Time and Space (Usio, Simidu, Ed.), pp. 141–147. Kluwer Academic Publishers, New York.
[31] Kjelleberg, S. and Hermansson, M. (1984) Starvation-induced effects on bacterial surface characteristics. Appl. Environ. Microbiol. 48, 497–503.
[32] Arrieta, J.M. and Herndl, G.J. (2001) Changes in bacterial β-glucosidase diversity during a coastal phytoplankton bloom. Limnol. Oceanogr. 47, 594–599.
[33] Gurijala, K.R. and Alexander, M. (1990) Effect of growth rate and hydrophobicity on bacteria surviving protozoan grazing. Appl. Environ. Microbiol. 56, 1631–1635.

[34] Matz, C. and Jürgens, K. (2001) Effects of hydrophobic and electrostatic cell surface properties of bacteria on feeding rates of heterotrophic nanaoflagellates. Appl. Environ. Microbiol. 67, 814–820.
[35] Bar-Or, Y. (1990) Hydrophobicity in the aquatic environment In: Cell Surface Hydrophobicity (Doyle, J. and Rosenberg, M., Eds.), pp. 211–229. ASM Press, Washington, DC.
[36] Eilers, H., Pernthaler, J., Gloeckner, F.O. and Amann, R. (2000) Culturability and in situ abundance of pelagic bacteria from the North Sea. Appl. Environ. Microbiol. 66, 3044–3051.
[37] Beardsley, C., Pernthaler, J., Wosniok, W. and Amann, R. (2003) Are readily culturable bacteria in coastal North Sea waters suppressed by selective grazing mortality?. Appl. Environ. Microbiol. 69, 2624–2630.